

Intrinsic and Extrinsic Galaxy Alignment

Paolo Catelan, Marc Kamionkowski and Roger D. Blandford

California Institute of Technology, Mail Code 130-33, Pasadena, CA 91125, USA

May 2000

ABSTRACT

We show with analytic models that the assumption of uncorrelated intrinsic ellipticities of target sources that is usually made in searches for weak gravitational lensing due to large-scale mass inhomogeneities (“field lensing”) is unwarranted. If the orientation of the galaxy image is determined either by the angular momentum or the shape of the halo in which it forms, then the image should be aligned preferentially with the component of the tidal gravitational field perpendicular to the line of sight. Long-range correlations in the tidal field will thus lead to long-range ellipticity-ellipticity correlations that mimic the shear correlations due to weak gravitational lensing. We discuss uncertainties (which are still considerable) in the predicted amplitude of this correlation, and consider several methods for discriminating between the weak-lensing (extrinsic) and intrinsic correlations, including the use of redshift information. An ellipticity-tidal-field correlation also implies the existence of an alignment of images of cluster-member galaxies in the outskirts of clusters. Although the intrinsic alignment may complicate the interpretation of field-lensing results, it is inherently interesting as it may shed light on galaxy formation as well as on structure formation.

Key words: cosmology: theory - gravitational lensing - large-scale structure

1 INTRODUCTION

Searches for weak gravitational lensing due to large-scale mass inhomogeneities are coming of age. Ellipticities of high-redshift sources are taken to be indicators of the shear field induced by weak gravitational lensing by mass inhomogeneities along the line of sight, and shear-shear correlations can be used as a probe of the lensing-mass distribution (Gunn 1967; Miralda-Escudé 1991; Blandford et al. 1991; Kaiser 1992; Bartelmann & Schneider 1992; Bartelmann & Schneider 1999). The advantage of weak lensing is that it determines the power spectrum (as well as higher-order statistics; e.g., Munshi & Jain 1999; Cooray & Hu 2000) for the *mass* rather than the light. In just the past few months, four groups have reported the first detections of such “field lensing” (Bacon, Refregier & Ellis 2000; Kaiser, Wilson & Luppino 2000; Wittman et al. 2000; van Waerbeke et al. 2000).

Noise for the weak-lensing signal is provided by the intrinsic ellipticities of the sources. With a sufficiently large sample of sources, the random orientation of these sources can be overcome. One thus looks for an ellipticity correlation in excess of the Poisson noise provided by randomly oriented intrinsic ellipticities. The analysis always assumes that the intrinsic orientations of the sources are entirely random and isotropically distributed. The point of this paper will be to demonstrate that this should not be the case.

To do so, we consider two *ansatzen* for the origin of

the ellipticity of the high-redshift sources. We first suppose that the orientation of the image is determined by the angular momentum of the halo in which it forms; this should be a good description if the sources are disk galaxies. The simplest hypothesis—adopted in nearly all disk-formation models (e.g., Dalcanton, Spergel & Summers 1997; Mo, Mao & White 1998; Buchalter et al. 2000)—is that the plane of the disk is perpendicular to the angular-momentum vector of the galactic halo in which the disk forms. According to linear perturbation theory, a galactic halo acquires its angular momentum via torquing of the aspherical protogalaxy in the tidal gravitational field that arises from the large-scale mass distribution (Hoyle 1949; Peebles 1969; Doroshkevich 1970; White 1984; Heavens & Peacock 1988; Catelan & Theuns 1996a). Averaging over all possible orientations of the protogalaxy, the disks are correlated with the tidal field. Alternatively, the ellipticity of the galaxy image may be determined primarily by the shape of the halo in which it forms; this might be expected if the sources are isolated ellipticals. In this case, a modification of the spherical-top-hat model for gravitational collapse in a tidal field also suggests a preferential elongation of the galaxies along the direction of the tidal field. Thus, in either case, the observed orientations of each source should be determined, at least in part, by the tidal gravitational field in which it lives. In this way, long-range correlations in the mass distribution will lead to long-range correlations in the inferred shear from these sources.

In the next Section, we review briefly the statistics used to describe the weak-lensing signal. In Section 3, we show how tidal torquing can align galaxies preferentially along the tidal gravitational field, and how this will lead to a preferred orientation for the projected image. Section 4 deals with elongation of ellipticals. Section 5 discusses the estimate of the constant of proportionality relating the inferred shear to the tidal field. Section 6 presents the calculation of the shear power spectrum. Section 7 presents numerical results. In Section 8 we put forth some ideas for disentangling the intrinsic and weak-lensing signals, including the use of redshift information, and we predict a corresponding alignment in the images of cluster-member galaxies in the outskirts of galaxy clusters. We close with some concluding remarks in Section 9.

During preparation of this paper, we learned of related work (using numerical simulations) by Heavens, Refregier & Heymans (2000) and Croft & Metzler (2000). Our analytic approach should complement their numerical work and perhaps help shed some light on the origin of their observed correlations. The analytic calculation should also be useful in determining the correlation at large angular separations, where it becomes increasingly difficult to measure in simulations. Our analytic approach also suggests some possible intrinsic/weak-lensing discriminators. In addition, we have learned of similar analytic work currently in preparation by Mackey & White (2000).

2 FORMALISM AND STATISTICS

As discussed, e.g., in Kamionkowski et al. (1998), weak lensing induces a stretching of images on the sky at position $\vec{\theta} = (\theta_y, \theta_z)$ described by ϵ_+ , the stretching in the $\theta_y - \theta_z$ directions, and ϵ_\times , the stretching along axes rotated by 45° (we take the line of sight to be the \hat{x} direction). Precise definitions for these “ellipticities” are discussed, e.g., by Blandford et al. (1991). The weak-lensing shear, $\gamma(\vec{\theta})$, can be recovered through its Fourier transform (Stebbins 1996),

$$\tilde{\gamma}(\vec{\ell}) = \frac{(\ell_y^2 - \ell_z^2)\tilde{\epsilon}_+(\vec{\ell}) + 2\ell_y\ell_z\tilde{\epsilon}_\times(\vec{\ell})}{\ell_y^2 + \ell_z^2}, \quad (1)$$

where $\tilde{\epsilon}_+(\vec{\ell}) = \int \vec{\theta} \epsilon_+(\vec{\theta}) e^{i\vec{\ell} \cdot \vec{\theta}}$, is the Fourier transform of the ellipticity (and similarly for the other quantities). Statistical homogeneity and isotropy guarantee that the Fourier coefficients, $\tilde{\gamma}(\vec{\ell})$, have zero mean and variances,

$$\langle \tilde{\gamma}^*(\vec{\ell})\tilde{\gamma}(\vec{\ell}') \rangle = (2\pi)^2 \delta(\vec{\ell} - \vec{\ell}') C(\ell), \quad (2)$$

where $C(\ell)$ is the weak-lensing power spectrum. The mean-square ellipticity (which is usually taken to be the mean-square shear) smoothed over some circular window of radius θ_p is

$$\langle (\gamma_g^s)^2 \rangle = \int \frac{d^2 \vec{\ell}}{(2\pi)^2} C(\ell) |\widetilde{W}(\vec{\ell})|^2, \quad (3)$$

where $\widetilde{W}(\ell) = 2J_1(x)/x$ is the Fourier-space window function, $J_1(x)$ is a Bessel function, and $x \equiv \ell\theta_p/\sqrt{\pi}$.

Two nonzero 2-point ellipticity-ellipticity correlation functions can be constructed from the two ellipticities, ϵ_+ and ϵ_\times , determined by taking the coordinate axes to be aligned with the line connecting the two correlated points.

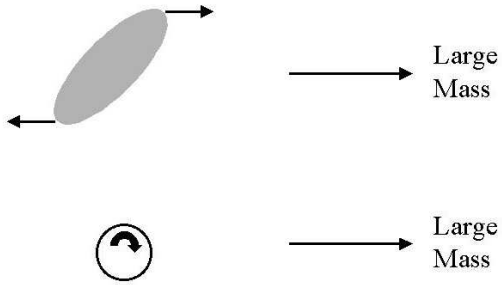


Figure 1. The upper panel shows a distant mass acting upon a prolate halo and causing it to start spinning as shown. The torque vanishes when $\theta = 0, \pi/2$, cf., Eq. 5. The lower panel shows that baryons in the potential well will fall in to form a disk lying in the plane of the figure. When this disk is viewed from the direction perpendicular to the figure, there will be no induced ellipticity; when viewed from the plane of the figure, the ellipticity will be ~ 1 . Averaging over all viewing directions gives a non-zero mean elongation of the galaxy image along the projected direction of the distant mass and this will be correlated among neighboring galaxies. More generally, tidal gravitational fields will be induced by the large-scale distribution of mass (rather than by a single large mass), and long-range correlations in these tidal fields will induce long-range correlations in the ellipticities of widely separated galaxies.

These correlation functions are $C_1(\theta) = \langle \epsilon_+^r(\vec{\theta}_0) \epsilon_+^r(\vec{\theta}_0 + \vec{\theta}) \rangle$ and $C_2(\theta) = \langle \epsilon_\times^r(\vec{\theta}_0) \epsilon_\times^r(\vec{\theta}_0 + \vec{\theta}) \rangle$, and they are given in terms of the power spectra by

$$\begin{aligned} C_1(\theta) + C_2(\theta) &= \int_0^\infty \frac{\ell d\ell}{2\pi} C(\ell) J_0(\ell\theta), \\ C_1(\theta) - C_2(\theta) &= \int_0^\infty \frac{\ell d\ell}{2\pi} C(\ell) J_4(\ell\theta), \end{aligned} \quad (4)$$

where $J_\nu(x)$ are Bessel functions.

3 TIDAL TORQUES AND IMAGE ORIENTATIONS

When the mass that will eventually collapse to form a galaxy breaks away from the expansion, it will in general have an anisotropic moment-of-inertia tensor $\mathcal{I}_{\alpha\beta}$ and reside in a tidal gravitational field $\mathcal{D}_{\alpha\beta} = \partial_\alpha \partial_\beta \phi$ generated by the larger-scale distribution of mass, where ϕ is the gravitational potential. The moment-of-inertia eigenframe will most generally not be aligned with the that of the tidal field. A net torque will thus be applied to the protogalaxy, and the galactic halo that results will have an angular momentum $L_\alpha \propto \varepsilon_{\alpha\beta\gamma} \mathcal{I}_{\beta\sigma} \mathcal{D}_{\gamma\sigma}$, where $\varepsilon_{\alpha\beta\gamma}$ is the Levi-Civita symbol (see Figure 1). The relation between the ellipticity and angular momentum will ultimately be determined empirically by fitting to the observed ellipticities (see Section 5 below), so the absolute magnitude of \mathbf{L} is irrelevant. Thus, when we refer to the “angular momentum” \mathbf{L} in the following, we will really be discussing a vectorial spin parameter, an angular momentum that has been scaled by the galaxy mass and binding energy to be dimensionless.

Let us assume that if a disk forms in a galactic halo, it will form in the plane perpendicular to the angular-

momentum vector. It is also reasonable to suppose that the ellipticity of a disk galaxy, viewed edge on, might depend on the magnitude of the angular momentum. If viewed at an inclination angle α , the ellipticity will be reduced by $\cos \alpha$. Taking the line of sight to be the $\hat{\mathbf{x}}$ axis, the observed ellipticity will be $\epsilon_+ = f(L)(L_y^2 - L_z^2)$ and $\epsilon_x = 2f(L)L_yL_z$, where $L = |\mathbf{L}|$. We will choose the function $f(L) = CL^{-1}$. This will guarantee that the fraction of the ellipticity that is subject to long-range correlations will be proportional to the fraction of the tidal field that is subject to long-range correlations. Thus, we set $\epsilon_+ = C(L_y^2 - L_z^2)/L$ and $\epsilon_x = 2CL_yL_z/L$. The constant of proportionality C will be determined below from the observed mean ellipticity of sources.

Let us now suppose that a number of galaxies form in the same tidal field. Since the angular momentum (and corresponding observed ellipticity) of a given galaxy will depend on the moment of inertia of its parent protogalaxy, the tidal field alone does not determine the orientation of a given disk. However, if the moment-of-inertia eigenframes are distributed isotropically, a net alignment of the galaxies with the tidal field remains after averaging over all initial moments of inertia.

To demonstrate this, we will consider a somewhat simplified model that should still capture the essential physics and leave out details (to be presented elsewhere; Catelan & Kamionkowski 2000). Rather than average over the entire distribution of moments of inertia—which can be obtained, e.g., from Gaussian peak statistics (Bardeen et al. 1986; Heavens & Peacock 1988; Catelan & Theuns 1996a)—we will suppose that each galaxy has the same eigenframe moment of inertia and that the eigenframes are distributed isotropically. Moreover, we will suppose that two of the three principal moments are equal. The unequal moment defines a symmetry axis $\hat{\mathbf{n}} = (\sin \theta \cos \varphi, \sin \theta \sin \varphi, \cos \theta)$, and the contributing part of the moment-of-inertia tensor is $\mathcal{I}_{\alpha\beta} \propto n_\alpha n_\beta$, where $\hat{\mathbf{n}} = (\sin \theta \cos \varphi, \sin \theta \sin \varphi, \cos \theta)$.

In the most general case, the tidal field $\mathcal{D}_{\alpha\beta}$ is a symmetric rank-3 tensor, with 6 free parameters. In the linear-theory power-spectrum calculation below, we will consider each Fourier mode independently. If we are considering only one Fourier mode \mathbf{k} of the gravitational potential, then the tidal-field tensor is $\mathcal{D}_{\alpha\beta} = -k_\alpha k_\beta \phi$. The induced angular momentum is thus $\mathbf{L} = (\hat{\mathbf{n}} \cdot \mathbf{k})(\hat{\mathbf{n}} \times \mathbf{k})\phi$ (up to a constant of proportionality to be dealt with below).

If \mathbf{k} is perpendicular to the line of sight, say in the $\hat{\mathbf{z}}$ direction, then the observed ellipticity of a galaxy that forms from a protogalaxy with symmetry axis in the $\hat{\mathbf{n}}$ direction is

$$\epsilon_+ = Ck^2 \phi |\sin \theta \cos \theta| \cos^2 \varphi, \quad \epsilon_x = 0. \quad (5)$$

So, for example, if the symmetry axis is aligned with ($\theta = 0$) or perpendicular to ($\theta = \pi/2$) the tidal field, there will be no torque. If the symmetry axis is in the x - z plane, then it will be torqued about the $\hat{\mathbf{y}}$ direction and the resulting image will be elongated in the $\hat{\mathbf{z}}$ direction. If the symmetry axis is in the y - z plane, the galaxy will spin about the line of sight and produce a face-on (zero-ellipticity) disk.

We now assume that the orientations of the protogalaxy eigenframe are random. In principle, the location and shapes of peaks from which the protogalaxy forms depend on all Fourier modes in the initial density field, including those that determine the long-range tidal field. However, we make the usual peak-background split. The small-scale fluctua-

tions that play the dominant role in determining the shape of the protogalaxy should be statistically independent of larger-scale fluctuations. Thus, the long-wavelength modes that give rise to long-range tidal-field correlations should not have any significant impact on the protogalaxy shape.

Integrating equation (5) over all angles, we find that the inferred shear, the mean ellipticity of galaxies formed in this tidal gravitational field, is $\epsilon_+ = Ck^2 \phi/6$, $\epsilon_x = 0$. Thus, although there is no one-to-one correspondence between the tidal gravitational field in which a galaxy forms and the orientation of the galaxy image, *on average, there will be a tendency for galaxy images to be aligned with the component of the tidal gravitational field perpendicular to the line of sight.*

Given that $k_\alpha \phi \propto i\partial_\alpha \phi$ and from the transformation properties of ϵ_+ and ϵ_x , it follows that for arbitrary \mathbf{k} perpendicular to the line of sight,

$$\begin{aligned} \epsilon_+ &= C(\partial_y^2 - \partial_z^2)\phi/6, \\ \epsilon_x &= 2C\partial_y\partial_z\phi/6. \end{aligned} \quad (6)$$

This is one of our central results.

Galaxies that form in a tidal field perpendicular to the line of sight will form edge-on disks, but their orientations will be isotropic thus leading to no induced shear. We can also consider more general directions for \mathbf{k} , but only Fourier modes perpendicular to the line of sight will produce angular shear correlations.

4 HALO SHAPE DISTORTIONS

Alternatively, we can postulate that the observed shape of a galaxy is determined by the shape of the halo rather than by its angular momentum; i.e., by its geometry rather than its dynamics. In this case, the observed ellipticity of a galaxy should still be related to the tidal field as in equation (6). Suppose a spherical overdensity undergoes gravitational collapse to form a galaxy in a region of constant tidal gravitational field. Then equipotential surfaces for the galaxy will be elongated (compressed) along the direction of the tidal gravitational field for positive (negative) tidal field. The resulting image will either be elongated in the same way as the halo, or a baryonic pancake may form in a plane perpendicular to the tidal field if that axis undergoes gravitational collapse first. Thus it is reasonable to expect heuristically that the luminous galaxy that forms will have an orientation partially determined by the tidal gravitational field in which it forms. Arguments similar to those given above for image shapes determined by angular momentum suggest that the observed ellipticity will generally depend on the tidal field as in equation (6), albeit with a different C . In this case, the signs of ϵ_+ and ϵ_x may depend on whether the halo is oblate or prolate, as well as on the halo orientation.

5 NORMALIZATION

Given an initial protogalaxy moment of inertia and tidal field, the angular momentum of a given halo can be calculated in linear theory (Heavens & Peacock 1988; Catelan & Theuns 1996a), with a result that is in reasonably good agreement with numerical simulations (Sugerman, Summers

& Kamionkowski 2000; Lee & Pen 2000). And in principle, the ellipticity of the luminous galaxy can be related to the halo angular momentum with a disk-formation model. However, current disk-formation models are not yet sophisticated enough to predict robustly the disk ellipticity from first principles; rather the models are constructed to provide a good fit to the observed disks. Given this state of affairs, we will empirically estimate the constant of proportionality C between the ellipticity and the tidal field.

To do so, we calculate the expected rms ellipticity of individual galaxies and then compare it with the typical source ellipticity to fix C . We use $\bar{\epsilon} \simeq 0.15$ (M. Metzger, private communication), although it might be larger for some high-redshift populations. We return to the relations $\mathbf{L} = (\hat{\mathbf{n}} \cdot \mathbf{k})(\hat{\mathbf{n}} \times \mathbf{k})\phi$, $\epsilon_+ = C(L_y^2 - L_z^2)/L$ and $\epsilon_\times = 2CL_yL_z/L$. Suppose first that the elongation of each galaxy is determined entirely by the moment of inertia of the protogalaxy and the tidal field in which it forms. Averaging over all orientations of \mathbf{L} , we find

$$\langle \epsilon^2 \rangle = \langle \epsilon_+^2 + \epsilon_\times^2 \rangle = \frac{8}{15} \langle \mathbf{L}^2 \rangle. \quad (7)$$

The expectation value of the square of the angular momentum comes from averaging over the orientations of $\hat{\mathbf{n}}$ and $\hat{\mathbf{k}}$ and then integrating over the power spectrum (Catelan & Theuns 1996a),

$$\begin{aligned} \langle \mathbf{L}^2 \rangle &= \langle [(\hat{\mathbf{n}} \cdot \nabla)(\hat{\mathbf{n}} \times \nabla)\phi]^2 \rangle \\ &= \frac{2}{15} \langle (\nabla^2\phi)^2 \rangle \\ &= \frac{2}{15} \int \frac{d^3\mathbf{k}}{(2\pi)^3} k^4 P_\phi(k), \end{aligned} \quad (8)$$

where $P_\phi(k)$ is the power spectrum for the gravitational potential which is related to the mass power spectrum $P(k)$, through the Poisson equation. We thus obtain

$$\langle \epsilon^2 \rangle = \frac{16}{225} C^2 \left(\frac{3}{2} \Omega_0 H_0^2 \right)^2 \frac{1}{2\pi^2} \int k^2 dk P(k) \left[\frac{3j_1(kR)}{kR} \right]^2. \quad (9)$$

This fixes the constant of proportionality C when we fix $\langle \epsilon^2 \rangle = \bar{\epsilon}^2 = (0.15)^2$. We have inserted a top-hat window function and choose to smooth over a radius $R = 1 \text{ Mpc } h^{-1}$, a characteristic scale over which a galaxy forms (tidal fields on smaller scales should not contribute to the torque). Below we will discuss how uncertainty in the smoothing scale will affect our final results.

6 SHEAR POWER SPECTRUM

In the absence of weak lensing, the shear measured in direction $\vec{\theta}$ will be the integrated shear along the line of sight,

$$\begin{aligned} \epsilon_+(\vec{\theta}) &= \int_0^\infty dx g(x) \epsilon_+(x, x\theta_y, x\theta_z) \\ &= \frac{C}{6} \int_0^\infty dx g(x) (\partial_y^2 - \partial_z^2) \phi(x, x\theta_y, x\theta_z), \end{aligned} \quad (10)$$

where $g(x)$ is the distribution of sources along the line of sight normalized to unity, and x is the comoving distance. We have assumed the Universe to be flat, as the cosmic microwave background seems to indicate (Kamionkowski, Spergel & Sugiyama 1994; Miller et al. 1999; de Bernardis

et al. 2000; Hanany et al. 2000). Using the generalized Limber's equation (Kaiser 1992), as well as the definition of γ in equation (1), we find

$$C(\ell) = (C/6)^2 \left(\frac{3}{2} \Omega_0 H_0^2 \right)^2 \int dx \frac{g^2(x)}{x^2} P(\ell/x). \quad (11)$$

If the ellipticity-ellipticity correlation evolves with time, then the time dependence of the mass power spectrum should be taken into account in the integrand. However, we are supposing that the ellipticity correlations are fixed by some primordial density field, so the time evolution does not matter. The overall normalization of $P(k)$ also does not matter, as this will be fixed below to match the observed source ellipticities.

Changing the variable of integration in equation (11) from x to k and inserting our expression for C , we get the intrinsic shear power spectrum,

$$C(\ell) = \frac{25\pi^2 \bar{\epsilon}^2}{32} \frac{1}{\ell} \frac{\int dk g^2(\ell/k) P(k)}{\int k^2 dk P(k) \left[\frac{3j_1(kR)}{kR} \right]^2}. \quad (12)$$

This expression bears some resemblance to that for weak gravitational lensing. The difference is that the $g(x)$ here is replaced by the distribution of lenses along the line of sight, and the normalization differs. All this should come as no surprise, since the shear produced by weak lensing also depends on the perpendicular components of the tidal field. Thus, barring the small difference expected from the different line-of-sight distribution, the angular dependence of the intrinsic correlation function should look quite a bit like that for weak lensing.

7 NUMERICAL RESULTS

Fig. 2 shows results for the shear power spectrum induced by intrinsic alignments as well as the power spectrum expected from weak lensing. Results are shown for a population of sources with a mean redshift $z_m \sim 1$ and a population with a mean redshift $z_m \sim 0.3$. The weak-lensing power spectrum is taken from Kamionkowski et al. (1998), and is for a cluster-abundance-normalized cold-dark-matter model.* The light dotted curves indicate how the intrinsic power spectrum (for the high-redshift population) would change if the smoothing scale for the normalization to the observed ellipticities was taken to be $R = 0.5 h^{-1} \text{ Mpc}$ (lower dotted curve) or $R = 2 h^{-1} \text{ Mpc}$ (upper dotted curve), instead of $R = 1 h^{-1}$.

The calculation indicates that for high-redshift sources, the intrinsic correlation is unlikely to dominate that from weak lensing. However, given the uncertainty in the normalization, and the approximation inherent in our calculation, we cannot rule out the possibility that the intrinsic correlation might be larger than our calculation has indicated. However, even if it is small, it is probably still large enough that it will need to be considered for cosmological-parameter estimation (e.g., Hu & Tegmark 1999) from future precise weak-lensing maps as well as for studies of higher-order statistics. The curves in Fig. 2 for the lower-redshift

* The amplitude of the weak-lensing power spectrum *does* depend on the amplitude of $P(k)$.

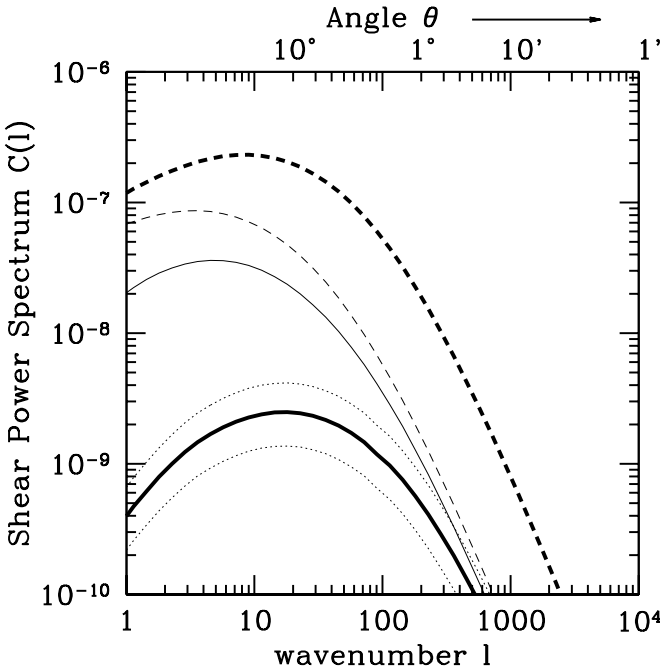


Figure 2. The angular shear power spectra for weak lensing (dashed curves) and for intrinsic alignments (solid curves) for a high-redshift source population with median redshift $z_m \sim 1$ (heavier curves) and a lower-redshift source population with $z_m \sim 0.3$ (lighter curves). The upper and lower dotted curves show the intrinsic power spectrum that would be obtained (for the high-redshift population) using a smoothing radius of $R = 2 h^{-1}$ Mpc or $R = 0.5 h^{-1}$ Mpc, respectively, instead of the nominal value of $R = 1 h^{-1}$. The mean source ellipticity is assumed here to be $\bar{\epsilon} = 0.15$, and the amplitude of the intrinsic power spectrum scales with $\bar{\epsilon}^2$.

population suggest that intrinsic alignment will be more important for weak-lensing searches with shallower surveys, such as the Sloan Digital Sky Survey and/or Two-Degree Field.

8 INTRINSIC VERSUS EXTRINSIC DISCRIMINATORS

8.1 Redshift information

Redshift information could be used to determine the relative contributions of the intrinsic and weak-lensing correlations. As Fig. 2 indicates, the weak-lensing signal is larger for more distant sources (as there is more line of sight for the signal to accrue), while the intrinsic correlation should actually increase for lower-redshift sources. We should caution, however, that dynamical processes might dilute intrinsic ellipticity correlations with time; this should be amenable to further study by numerical simulations. It is thus plausible that low-redshift populations show no intrinsic correlation even though high-redshift populations do.

Another possibility would be to exploit the different dependence of the weak-lensing and intrinsic correlations on the redshift distribution of the sources. Since the weak-lensing signal accrues along the line of sight, the ellipticity correlation between two objects nearby on the sky but

widely separated in redshift may be significant. On the other hand, the intrinsic ellipticity correlation should be larger for pairs of sources that are close in redshift. Some indication of this can be seen in equation (11). Consider a distance distribution $g(x)$ that is a top hat centered at x_0 with width Δx . The shear power spectrum that results is inversely proportional to Δx (as long as Δx is not so small that the approximation used in deriving equation (11) breaks down).

Along similar lines, our model predicts the existence of correlations between ellipticities of spatially close pairs of galaxies. Redshift surveys should yield a good sample of close (in redshift as well as celestial position) pairs of galaxies with which this correlation could be searched.

8.2 Cuts on Intrinsic Ellipticities

The strength of the shear induced by weak-lensing does not depend on the intrinsic ellipticities of the sources. On the other hand, our calculation [cf. equation (12)], suggests that the magnitude of the intrinsic correlation is proportional to the square of the average ellipticity of the sources. Thus, the intrinsic correlations could be reduced by using sources with smaller intrinsic ellipticities, or by choosing isophotes that yield images of the smallest intrinsic ellipticity. Alternatively, one could determine the ellipticity correlation functions for the same population of sources, but using several different isophotes. Since the weak-lensing signal should not depend on the intrinsic ellipticity while the intrinsic correlation should, comparison between these various correlation functions can be used to separate the intrinsic and weak-lensing signals in much the same way that multifrequency cosmic-microwave-background maps disentangle the cosmological signal from Galactic foregrounds.

8.3 Cross-correlation with density

Another possibility is cross-correlation between the shear and the convergence. In addition to distorting images, weak lensing will also affect the density of sources on the sky, and this might be used to isolate the weak-lensing signal. However, given that the tidal field is correlated with the mass (and thus the galaxy) distribution, there may be a similar cross-correlation between the density of sources and the intrinsic orientations that should be investigated further.

8.4 Intrinsic correlations around clusters

Our model makes a precise prediction for the relation between the mean orientation of galaxies and the tidal field in which they form. Clusters produce significant tidal fields (in the radial direction) that can be determined fairly reliably from mass maps derived from weak lensing, dynamics, and x-ray observations. The algorithms that have been developed to look for alignment of distant background galaxies due to weak lensing by the cluster could be applied to the *cluster-member galaxies* in the outer regions of clusters to search for an alignment with the tidal field. If the alignment is too small to be detectable with the finite number of galaxies associated with one cluster, it may be possible to “stack” several clusters to improve the sensitivity to this alignment.

This ought to provide an alternative and possibly superior calibration of the intrinsic alignment.

9 CONCLUSIONS AND DISCUSSION

We have shown that the angular momenta and/or shapes of galactic halos should depend to some extent on the tidal gravitational field in which they are produced. Long-range correlations in the gravitational field should thus lead to long-range correlations in the shear inferred from images of distant galaxies. Although uncertainties in the relation between the luminous-galaxy shape and the halo prohibit us from carrying out a “first principles” calculation of the correlation, we can estimate the magnitude of the correlation by calibrating to the observed distribution of ellipticities.

The amplitude of the intrinsic power spectrum is increased (decreased) with a larger (smaller) smoothing length R . Realistically, there will be factors in addition to those that we have considered that contribute to the observed orientation, and these could decrease the correlation. For example, major mergers could affect both the halo angular momentum as well as the spin of the disk relative to that of the halo. Nonlinear corrections may play some role (Catelan & Theuns 1996b), and numerical simulations do indeed show some scatter between the direction of the halo angular momentum and that predicted by the linear theory (Sugerman, Summers & Kamionkowski 2000). Likewise, if the luminous-galaxy orientation is determined by the halo shape, the moment of inertia of the protogalaxy (which we have assumed is independent of the tidal field) will play a role in determining the orientation of the galaxy.

All of these effects will tend to diminish the correlations predicted by our model. However, results from numerical simulations (Heavens, Refregier & Heymans 2000; Croft & Metzler 2000) seem to indicate that the correlations in the halos have not been too diluted by these effects. Although these simulations quantify the correlations of the parent halos, there is still a considerable amount of physics relating the halo shape to the shape of the luminous galaxy that cannot yet be described properly with simulations. Heuristically, these effects should tend to diminish the intrinsic correlations even further. If future theoretical work determines that the degradation is considerable, then the effects we are discussing will be unimportant for interpretation of recent field-lensing detections. However, even if the correlation is small, it should not be zero—we have indeed identified realistic physical effects that should play at least some role in aligning galaxy images. Thus, the physical effects we have discussed here will be important for interpretation of and cosmological-parameter estimation from future more precise weak-lensing maps, as well as for understanding the implications of measurements of higher-order statistics.

At first, this intrinsic correlation may be seen as a nuisance for field-lensing searches. However, the intrinsic correlation arises from the same long-range correlations in the density field that give rise to the weak-lensing correlation. Moreover, the galaxy-formation physics that produces spins and shapes of galaxies is itself inherently interesting. Thus, measurement of these intrinsic correlations would be of fundamental significance for structure formation and galaxy formation.

ACKNOWLEDGMENTS

We thank D. Bacon, R. Croft, R. Ellis, M. Metzger, C. Metzler, A. Refregier, and M. White for discussions. This work was supported in part by NSF AST-9900866, AST-0096023, NASA NAG5-8506, and DoE DE-FG03-92-ER40701.

REFERENCES

Bacon D., Refregier A., Ellis R. S., 2000, astro-ph/0003008
 Bardeen J. M., Bond J. R., Kaiser N., Szalay A. S., 1986, ApJ, 304, 15
 Bartelmann M., Schneider P., 1992, A&A, 259, 413
 Bartelmann M., Schneider P., 1999, astro-ph/9912508
 Blandford R. D., Saut A. B., Brainerd T. G., Villumsen J. V., 1991, MNRAS, 251, 600
 Buchalter A., Jimenez R., Kamionkowski M., Heavens A., 2000, in preparation
 Catelan P., Kamionkowski M., 2000, in preparation
 Catelan P., Theuns T., 1996a, MNRAS, 282, 436
 Catelan P., Theuns T., 1996b, MNRAS, 282, 455
 Cooray A., Hu W., 2000, astro-ph/0004151
 Croft R., Metzler C., 2000, astro-ph/0005384
 Dalcanton J., Spergel D. N., Summers F. J., 1997, ApJ, 482, 659
 de Bernardis P. et al., 2000, Nature, 404, 955
 Doroshkevich A. G., 1970, Afz, 6, 581
 Gunn J. E., 1967, ApJ, 150, 737
 Hanany S. et al., 2000, astro-ph/0005123
 Heavens A. F., Peacock J. A., 1988, MNRAS, 243, 133
 Heavens A., Refregier A., Heymans C., 2000, astro-ph/0005269
 Hoyle F., 1949, in Burgers J. M., van de Hulst H. C., eds., in Problems of Cosmical Aerodynamics (Dayton, Ohio: Central Air Documents), p. 195
 Hu W., Tegmark M., 1999, ApJ, 514, L65
 Kaiser N., 1992, ApJ, 388, 272
 Kaiser N., Wilson G., Luppino G. A., 2000, astro-ph/0003338
 Kamionkowski M., Spergel D. N., Sugiyama N., 1994, ApJ, 426, L57
 Kamionkowski M., Babul A., Cress C., Refregier A., 1998, MNRAS, 301, 1064
 Lee J., Pen U.-L., 2000, ApJ, 532, L5
 Mackey J., White M., 2000, in preparation
 Miller A. D. et al., 1999, ApJ, 524, L1
 Miralda-Escudé J., 1991, ApJ, 380, 1
 Mo H. J., Mao S., White S. D. M., 1998, MNRAS, 297, L71
 Munshi D., Jain B., 1999, astro-ph/9911502
 Peebles P. J. E., 1969, ApJ, 155, 393
 Stebbins A., 1996, astro-ph/9609149
 Sugerman B., Summers F. J., Kamionkowski M., 2000, MNRAS, 311, 762
 van Waerbeke L., 2000, astro-ph/0002500
 Witmann D. A. et al., 2000, astro-ph/0003014
 White S. D. M., 1984, ApJ, 286, 38